MEASUREMENT OF SOLUTE DIFFUSIVITY IN ELECTRICALLY CONDUCTING LIQUIDS

T. ALBOUSSIÈRE
Department of Engineering
University of Cambridge
Trumpington Street, Cambridge CB2 1PZ

J.P. GARANDET
Commissariat à l'Énergie Atomique, DTA/CEREM/DEM
LRBS au CENG, 38054 Grenoble Cedex 9

AND

P. LEHMANN AND R. MOREAU
Laboratoire EPM-Madylam, CNRS UPR A 9033
ENSHMG BP 95, 38402 Saint Martin d'Hères

Abstract. The use of a magnetic field in the measurement of diffusion coefficients in liquid metals or semi-conductors is analyzed. Previous studies have demonstrated the disturbing influence of buoyancy-driven convection on the species transport in the shear-cell technique. A theory of effective diffusivity was proposed to account for the convective part of the transfer (GBD95). The idea developed here is to combine this effective diffusivity with the Lorentz electromagnetic damping of convection. The expected influence of the magnetic field is that the convective contribution should scale as Ha^{-4}. Experiments were carried out and, for a small convection level, this magnetic influence was confirmed. It is suggested that a strong steady magnetic field could enable the precise measurement of liquid metal alloys diffusivities. The present analysis gives the required magnetic field magnitude.

1. Introduction

For two independent reasons, it is important to measure accurately the chemical diffusivities in liquid metals. Firstly, some fundamental studies

A. Alemany et al. (eds.),
Transfer Phenomena in Magnetohydrodynamic and Electroconducting Flows, 359–372.

of the structure of liquid metal could use precise measurements to select one diffusion theory among all of them. Secondly, precise values are now needed to feed the powerful modelling methods in crystal growth or metallurgy. However, due to the extremely small values of these solute diffusivities of order $10^{-9}m^2.s^{-1}$, any attempt to measure them is a challenge: during an experiment of diffusion where the liquid is supposed to be at rest, a small reminiscent motion is likely to contribute more to the mass transfer than pure diffusion itself (GBD95; ARR96; HR86). The method of the long capillary seems to be the most widely used and this paper addresses the question of the influence of parasitic convection during its application. The compositions being assumed small[1], the undesirable motion takes its origin in thermal buoyancy forces. A careful thermal design of the experimental device helps reducing these forces. Nevertheless, it has been necessary to carry out measurements in the microgravity environment to obtain reasonably precise diffusivity values for some alloys. Another approach is investigated here, relying on the damping of the movements in an electrically conducting liquid that a steady magnetic field should induce. After a presentation of the experimental technique in section (2), the model of effective diffusivity (first presented in (GBD95)) aiming at modelling the mass transport induced by convection will be recalled (section 3). How a magnetic field damps the convective contribution to mass transport is analyzed in (4) in the framework of the effective diffusivity. Section (5) is devoted to our recently started experimental program and section (6) to a discussion of the use of magnetic fields for the purpose of measuring precise values of solute diffusivities.

2. The shear cell technique

In a purely diffusive transfer, the mass transfer density field $\mathbf{J}$ is modelled by Fick's law in the limiting case of dilute alloys: $\mathbf{J} = -\rho D \nabla c$, where ρ, D, c denote the constant and uniform density, solute diffusivity and solute concentration expressed in mass fraction respectively. A configuration is settled in such that a one dimensional diffusion is expected. The initial state is a step function of concentration along the axis where diffusion will proceed, which we denote the x-axis. The conservation of solute mass ρc along with the expression of the diffusion flux $\mathbf{J}$ leads to a local equation of conservation in the x direction: $\rho \partial c/\partial t + \partial J_x/\partial x = 0$, where J_x is the single non zero component of $\mathbf{J}$. The solution of this local equation is well

[1]This is the so-called dilute approximation

known since the 19th century results in heat transfer and is an erf function

$$c(x,t) = c_1 + \frac{c_2 - c_1}{2}\left[1 + erf\left(\frac{x}{2\sqrt{Dt}}\right)\right], \tag{1}$$

when the initial condition is $c = c_1$ for $x < 0$ and $c = c_2$ for $x > 0$. The knowledge of the composition at a time T enables to derive the diffusivity.

The originality of the shear cell technique (see figure 1) initially proposed at the CEREM (Pra89), is aimed at creating the conditions of one-dimensional diffusion from a step function and at providing the possibility of "freezing" the composition function at a time T, determined by the operator. A thin capillary of diameter of order 1 mm is formed by the alignment of a number of discs where an eccentric circular hole has been drilled . The material of the discs forms then the boundary of the long capillary. All the discs are liable to rotate around a common central axis. Three configurations are needed during a measurement experiment. Firstly, the long capillary is split in two half capillaries, allowing their filling with the alloy at different compositions. Secondly, the full capillary should be formed, creating the initial step function. Thirdly, after a duration T of diffusion prescribed by the operator, all fractions of the capillary should be isolated, *e.g.* by rotating every other disk. How these steps can be performed is a matter of subtle technology. After the last step, the temperature is decreased to room temperature and the solid elementary alloy samples contained in each disk are globally analyzed. The mean value of the axial solute distribution on each disc length after a diffusion duration T is obtained. By comparison with the solution (1), an experimental value of diffusivity D is derived.

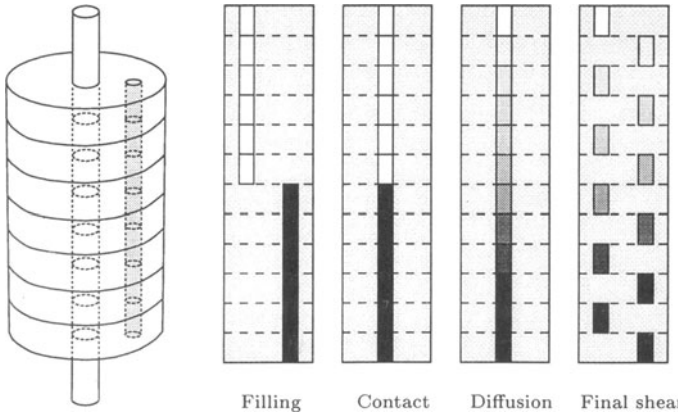

Figure 1. Shear cell sketch and principle

The figure 2 shows the evolution of the purely diffusive concentration profile given by the expression 1. Typically, the distance over which the composition gradient is spread scales as $\sqrt{Dt}$ with time.

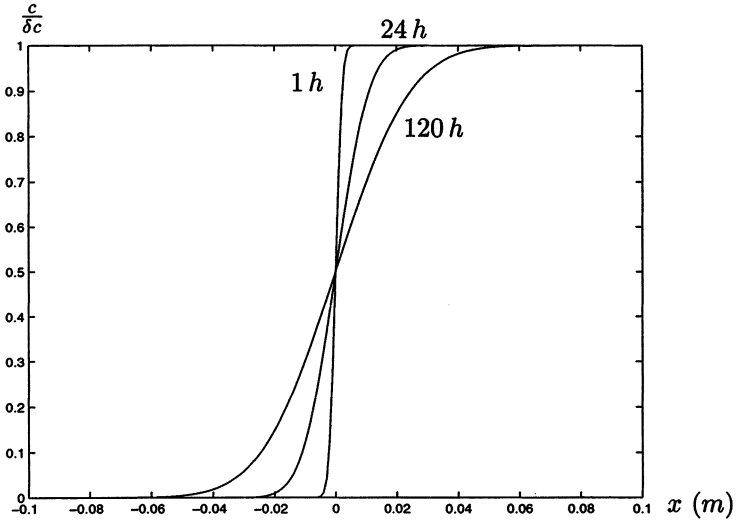

Figure 2. Pure diffusion profiles for SnBi after 1 hour, 24 hours and 120 hours ($D = 1.5 \times 10^{-9}\, m^2.s^{-1}$)

3. Convection and effective diffusivity

The previous section describes the ideal purely diffusive case. In this section, the effect of a weak convection on mass transport is addressed. A steady divergence free velocity field $\mathbf{v}$ is supposed to take place in the capillary with a zero normal component at the boundaries. In comparison with earlier works in the field, it is not necessary to suppose that the flow is one-dimensional. Nevertheless its variations in the direction of the x axis are assumed to take place on a larger length scale than the capillary diameter.

Fick's law for solute transfer holds in the reference system where matter is at rest. When expressed in the laboratory system of reference, it becomes $\mathbf{J} = -\rho D \nabla c + \rho c \mathbf{v}$, in the presence of convection. It remains possible and enlightening to express a local solute conservation equation along x. The basic experimental observable is the mean value of the concentration in the plane orthogonal to the x-axis at a given coordinate x, denoted $c_0(x,t)$, while the variations of concentration within this plane are represented by $c_1(x,y,z,t) = c(x,y,z,t) - c_0(x,t)$. The conservation of species along x takes the form $\rho\, \partial c_0/\partial t + \partial < J_x > /\partial x = 0$, where $< >$ denotes the average in the plane perpendicular to the x axis. A zero net global mass flux being

assumed in the x direction, because the fluid is confined in a closed cavity, it is not difficult to derive the following form $< J_x >= -\rho D\,(\partial c_0/\partial x) + \rho < v_x c_1 >$, where v_x is the x component of the velocity field. The solute equation along x can now be written

$$\frac{\partial c_0}{\partial t} = D\frac{\partial^2 c_0}{\partial x^2} - \frac{\partial < v_x c_1 >}{\partial x}. \tag{2}$$

It is clear from equation (2) that the field c_1 has to be considered in order to obtain a proper equation for c_0. The local point-wise solute conservation equation is $\rho\,\partial c/\partial t + div\,\mathbf{J} = 0$, which can be expanded as $\partial c/\partial t + \mathbf{v}.\nabla c = D\,\Delta c$. Hopefully, the difference between this isotropic equation and the x equation (2) should essentially involve c_1, the variation of the composition in the plane perpendicular to the x axis

$$\frac{\partial c_1}{\partial t} + \mathbf{v}.\nabla c_0 + \mathbf{v}.\nabla c_1 - \frac{\partial}{\partial x} < v_x c_1 > - D\,\Delta c_1 = 0. \tag{3}$$

Our primary goal being the analysis of the departure of species transfer from the purely diffusive case, we will treat convection as a small parameter. We can anticipate that the perturbation $\mathbf{v}$ is at the origin of a field c_1 of the same order, and both $\mathbf{v}.\nabla c_1$ and $(\partial/\partial x) < v_x c_1 >$ are second order terms in (3) compared to $\mathbf{v}.\nabla c_0$. For a weak convection it is also safe to neglect the first term $\partial c_1/\partial t$ in comparison with $D\,\Delta c_1$: these terms should be comparable if only axial variation was looked at, but by definition of c_1, and due to the aspect ratio of the cell, its variations in the cross-section are very large compared to its axial variation[2]. The first order disturbance form of (3) is

$$\Delta_S c_1 = D^{-1} v_x \frac{\partial c_0}{\partial x}, \tag{4}$$

where Δ_S denotes the Laplacian operator in the cross section and where ∇c_0 was replaced by its single non zero component $\partial c_0/\partial x$. The field c_1 must satisfy a zero normal gradient at the circular boundary. The solution of equation (4) is $f\,D^{-1}\partial c_0/\partial x$, where f is solution of $\Delta_S f = v_x$ and admits a zero normal gradient on the boundary. Using that result, the term $< v_x c_1 >$ takes the form $< v_x f > D^{-1}\,\partial c_0/\partial x$ and the basic equation for c_0 (2) can be written

$$\frac{\partial c_0}{\partial t} = \frac{\partial}{\partial x}\left[\left(D - \frac{< v_x f >}{D}\right)\frac{\partial c_0}{\partial x}\right]. \tag{5}$$

[2]Here is also made use of the assumption that the axial scale of variation of convection is much larger than the diameter.

The term in brackets is called an effective diffusivity (GBD95), $D_{eff} = D - < v_x f > /D$, by analogy of (5) with a diffusion equation. In the case of a fully-established convection along the axis, the effective diffusivity is independent of x and the equation governing c_0 becomes strictly identical to that of pure diffusion: given an experimental measurement of a diffusivity, it is impossible to guess what part of it is due to convection (see (GPVVA97)).

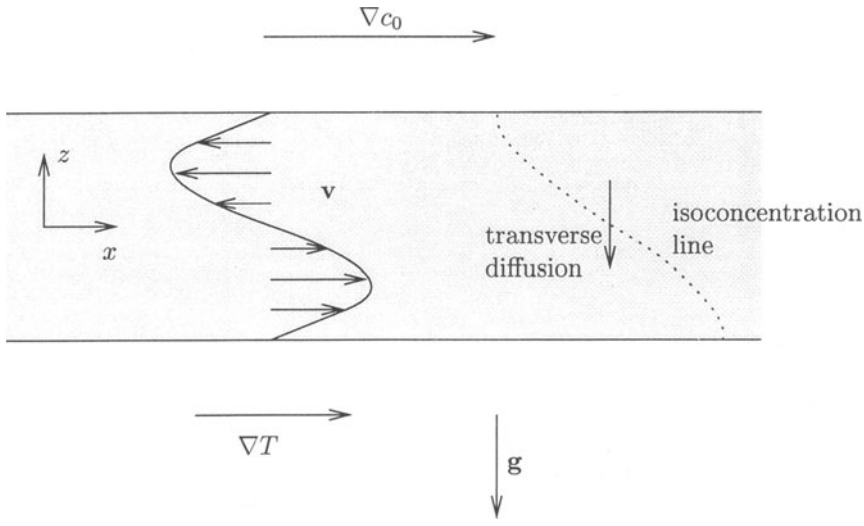

Figure 3. Convection in the capillary and the associated curvature of the iso-concentration lines

Some characteristics of the effect of convection on the apparent diffusivity (see equation 5) are now discussed (see reference (GBD95) for the original presentation of the effective diffusivity). It should be noted first that the term $< v_x f >$ is quadratic in the velocity. Indeed, because of the simple equation $\Delta_S f = v_x$, the function f depends linearly on the velocity v_x. A simple physical explanation can be given for the reason why the convection dimensionless parameter intervenes to the square in the expression of the effective diffusivity. The velocity field acts linearly on the mean axial concentration gradient $\partial c_0/\partial x$ to produce a lateral concentration difference. The convective transport contribution $< v_x c_1 >$ is then the product of the convective velocity by the lateral concentration. It is also striking that the convective contribution is inversely proportional to the "true" diffusivity D. This is related to how the lateral concentration difference is created. The interaction between the velocity field and the axial concentration gradient is a production term of lateral concentration, whereas lateral diffusion tends to limit the lateral concentration differences. So the equilibrium lat-

eral concentration is inversely proportional to D and so is the convective transport contribution to the overall transport.

4. Effect of a magnetic field

A simple configuration is now specified: the capillary of diameter H is assumed to be horizontal and an axial uniform temperature gradient G is supposed to exist (see figure 3). It has been shown in (GAM92), that this configuration was analogous to a vertical capillary in a transverse temperature gradient, since only the curl of the buoyancy driving force is to be considered. Let us denote z the direction opposite to the gravity vector and y the orthogonal direction to the x and z axis. The solution of the fully-established[3] buoyancy driven convective flow in the cylindrical cell is (Bej84)

$$v_x = \frac{Gr\,Sc}{32}\left[4Z^3 + 4ZY^2 - Z\right]\frac{D}{H}, \tag{6}$$

where $Z = z/H$, $Y = y/H$ and $Gr\,Sc = (\beta\, g\, G\, H^4)/(\nu\, D)$ can be considered as the product of a Grashof number and a Schmidt ν/D number (β, g and ν denote the volume expansion coefficient, gravity and the kinematic viscosity, respectively). Following the previous section analysis, the disturbance c_1 is derived analytically as the solution of a 2D harmonic equation and the resulting effective diffusivity is determined analytically , and the mean value of its product with v_x is exactly calculated

$$c_1 = \frac{\partial c_0}{\partial x} H \frac{Gr\,Sc}{768}\left[4Z^5 + 8Y^2Z^3 - 3Z^3 + 4Y^4Z - 3Y^2Z + Z\right]. \tag{7}$$

Equation (5) admits the following expression

$$\frac{\partial c_0}{\partial t} = D\left[1 + \frac{7\,(Gr\,Sc)^2}{11796480}\right]\frac{\partial^2 c_0}{\partial x^2}. \tag{8}$$

$$D_{eff} = D\left[1 + \frac{7\,(Gr\,Sc)^2}{11796480}\right]. \tag{9}$$

[3]The question of the stability of this flow is not relevant since inertia is likely to be negligible. We are indeed interested in regimes for which the effective diffusivity is not massively larger than the molecular diffusivity $D_{eff} \sim D$ and it was shown (GPVVA97) that the convective contribution to D_{eff} is of order DPe^2, where $Pe = VH/D$ is the solutal Péclet number. The kinematic viscosity being much larger than the species diffusivity for liquid metals and semiconductors, the Reynolds number VH/ν will be much smaller than unity if we restrict the analysis to Péclet numbers of order unity or less.

The increase of the effective diffusivity is quadratic in the governing non dimensional parameter $Gr\,Sc$.

In the same configuration, a transverse uniform vertical magnetic field is applied. When its magnitude B is such that the Hartmann number $Ha = \sqrt{\sigma/(\rho\nu)}BH$ (where σ denotes the electrical conductivity) is very large compared to unity, the convective velocity profile for electrically insulating boundaries tends towards (AGM93)

$$v_x = -\frac{Gr\,Sc}{Ha^2}\,2\,Z\,\frac{D}{H}, \tag{10}$$

except in the small Hartmann layer of typical thickness $Ha^{-1}H$ at the boundary. and the analytical derivation of D_{eff} yields now

$$c_1 = \frac{\partial c_0}{\partial x}\,H\,\frac{Gr\,Sc}{16\,Ha^2}\left[4\,Z^3 + 4\,Y^2 Z - 3\,Z\right]. \tag{11}$$

The equation of effective diffusivity (5) becomes now

$$\frac{\partial c_0}{\partial t} = D\left[1 + \frac{7\,(Gr\,Sc)^2}{384\,Ha^4}\right]\frac{\partial^2 c_0}{\partial x^2}. \tag{12}$$

$$D_{eff} = D\left[1 + \frac{7\,(Gr\,Sc)^2}{384\,Ha^4}\right]. \tag{13}$$

The magnetic field reduces the convective part of the effective diffusivity as Ha^{-4}, which makes it a quite promising tool to achieve good measurements on earth with the shear cell technique.

5. Our experimental program

In EPM-Madylam, an experimental device, EURIDICE, has been designed for the measurement of diffusivities using the shear cell technique under magnetic fields up to $0.75\,Tesla$. Contrary to many other experiments where thermal buoyancy forces are made as small as possible, a small constant temperature gradient (of order $0.5\,K.cm^{-1}$) is created so that the driving force is known. In order to achieve both temperature homogeneity or constant axial temperature gradients, the cells are placed into a graphite cylinder heated by three heating elements. An insulating material is placed around the graphite (Microtherm, $K = 0.03\,W.m^{-1}.K^{-1}$ at $500\,^oC$) and the external envelope is maintained at a constant temperature by a thermally regulated water circulation. The heating element in the middle compensate radial losses and the elements at each end prevent from axial losses.

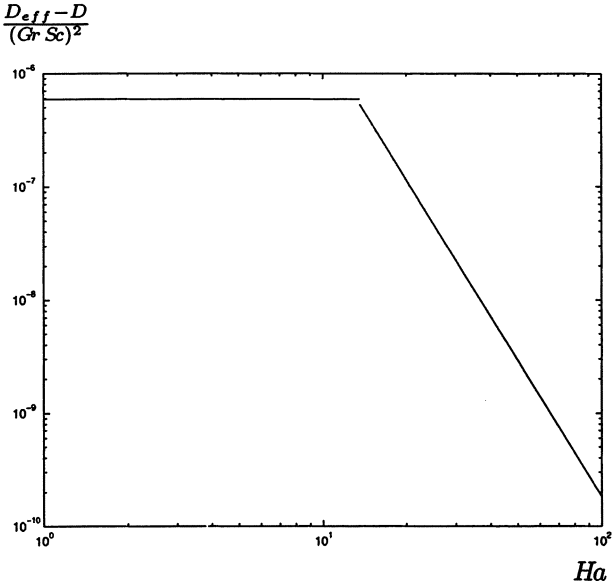

Figure 4. Dependence of the effective diffusivity on the Hartmann number. The transition between expression 9 without magnetic field and expression 13 for strong magnetic fields, occurs for a Hartmann number around 13.

Temperature measurements are made with thermocouples passed through both the graphite cylinder and a hole in the shear cells. When equilibrating carefully the three heating elements, a $0.03\,^oC$ homogeneity is possible at $250\,^oC$ along the $20\,cm$ long capillaries. On one side, a piece of metal links the graphite cylinder to the water cooled external envelope. It allows heat losses : a perfect axial and linear temperature gradient can then be created by increasing the regulation temperature on one side and decreasing it on the other. The whole device is held by a vibration insulated support and placed in an electromagnet. Vertical magnetic fields up to $0.75\,T$ can then be applied.

The tin bismuth alloy, with low concentration in bismuth, has been one of the studied alloys (see figure 5). A concentration of $0.5\,at.\%$ of bismuth was put on one half and pure tin on the other half capillary. Despite this low concentration, it was found that solute-buoyancy effects were more important than thermal-buoyancy forces by a factor ten. In that case, the previous analyses does not apply directly, because the driving force of the flow depends on the axial solute gradient, which evolve in time when diffusion proceeds. Here follows a modification of the analysis developed in section 3 to this case. Concerning the concentration analysis, the equations are unchanged up to equation 4. The only difference is that the velocity appearing is due to solute buoyancy forces rather than thermal effects. Let

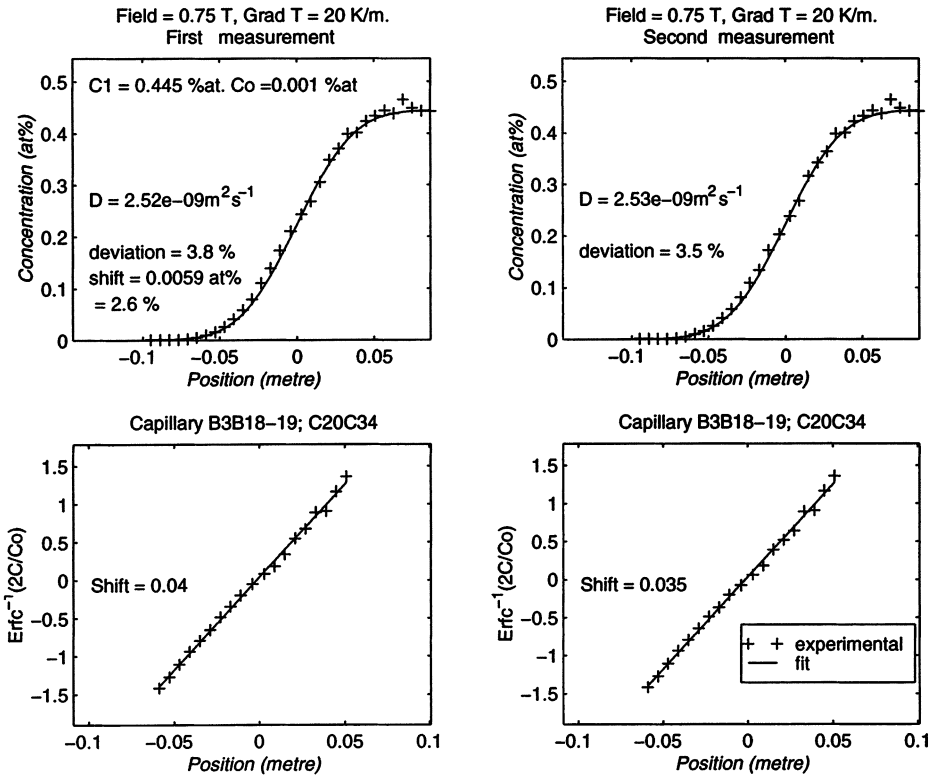

Figure 5. Concentration profile and associated erf function for SnBi at $0.5\,at\%$ in the horizontal configuration under a vertical magnetic field of magnitude $0.75\,T$.

us introduce a solute Grashof number,

$$Gr_c = \frac{\beta_c g \frac{\partial c_0}{\partial x} H^4}{\nu D}$$

where β_c is the compositional expansion coefficient of the alloy. This Grashof number depends on the axial concentration gradient, that depends on the axial position and on time. Nevertheless, the velocity driven by solute buoyancy forces takes the same form as previously where Gr_c is substituted to Gr. Equation 5 is still valid, but the convective contribution will now depend implicitly on the axial coordinate x through $\partial c_0/\partial x$ A difference appears when the corresponding expression to 8 is derived. A multiplicative factor 3 results from the variation of Gr_c with x. Without magnetic field, it is found that the axial concentration satisfies the following equation:

$$\frac{\partial c_0}{\partial t} = D\left[1 + \frac{21\,(Gr_c\,Sc)^2}{11796480}\right]\frac{\partial^2 c_0}{\partial x^2}. \qquad (14)$$

and under the condition of a large Hartmann number, we find the expression:

$$\frac{\partial c_0}{\partial t} = D\left[1 + \frac{21\,(Gr_c\,Sc)^2}{384\,Ha^4}\right]\frac{\partial^2 c_0}{\partial x^2}. \tag{15}$$

These two equations are more difficult to handle because they are non-linear ($\partial c_0/\partial x$ appears in Gr_c) and can not be characterized by a uniform and constant effective diffusivity. Instead, the effective diffusivity varies along the capillary (being maximum at the center where composition gradients are maximum) are evolves in time (decreasing in time because the initial composition step is smoothed). Nevertheless, the results showed clearly an effect of the magnetic field. The effective diffusivity measured seems almost uniform and decreased with increasing the magnitude of the magnetic field. The Gr number can be roughly estimated by a sort of averaged value. We have access to a composition gradient at the end of the experiment (which is the minimum over the experiment), but we can consider it at the middle of the capillary (where it is maximum). It is hoped that this composition gradient will be characteristic of the typical solute buoyancy driven forces during the whole experiment. It is estimated that the thermal Grashof number is $Gr \sim 5$, whereas the solute Grashof number is $Gr \sim 44$. Clearly, solute buoyancy forces dominate. In the absence of magnetic field, the associated effective diffusivity is enormous, and indeed the experiments showed a complete homogeneity of the composition. With $B \sim 0.75\,T$ (corresponding to a Hartmann number of 52 for a $2\,mm$ capillary), the effective diffusivity estimated is (with $Sc \sim 150$)

$$D_{eff} = 1.33 \times D. \tag{16}$$

Considering that the reference value is around $D = 1.5 \times 10^{-9} m^2.s^{-1}$ for SnBi, we predict an effective diffusivity around $2.26 \times 10^{-9} m^2.s^{-1}$, not far from the measured $2.52 \times 10^{-9} m^2.s^{-1}$, on figure 5. On figure 5 is also plotted the erf^{-1} function that shows that the compositional profile is not far from an erf function, despite the fact that the effective diffusivity is not strictly a constant.

On the figure 6 is plotted the value of the measured diffusivity coefficient versus the different values of the solutal Grashof-Schmidt product squared divided by the Hartmann number to the power four. The measured diffusivity increases with the this convective parameter. When this parameter is relatively small, the effective diffusivity theory developed above can be applied and a linear fit of the first points allows us to prolongate the curve at the origin, which should correspond to the purely diffusive case. The value found $D = 1.66 \times 10^{-9} m^2.s^{-1}$ is very close to the reference micro-gravity

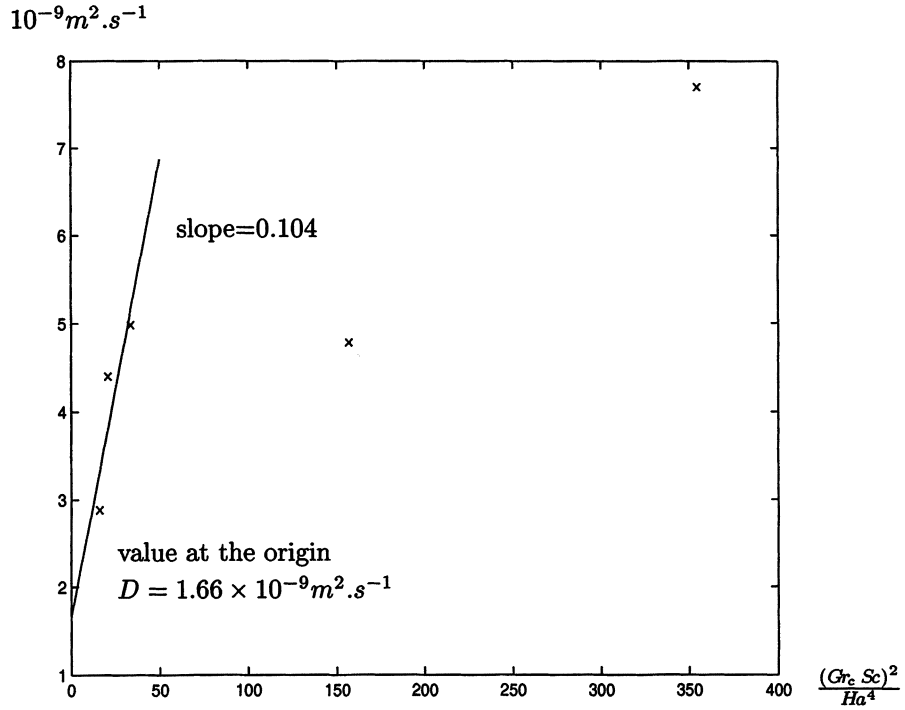

Figure 6. Measured diffusivities for different convective coefficients $\frac{(Gr_c\ Sc)^2}{Ha^4}$

value $1.5 \times 10^{-9}m^2.s^{-1}$. It should be noted that for this solute buoyancy-driven case, the measured diffusivity becomes smaller than the predicted effective diffusivity at high value of the parameter $Gr\ Sc/Ha^4$. An explanation to this behaviour is still to be found and might be connected to some solutal stratification effect that would damp the flow, somehow similar to the stratification mechanism in the vertical configuration (Har71).

Other experiments have been carried out with another alloy, SnIn. An interesting property of this alloy is that its density does not depend very much with composition. Only the thermal buoyancy forces should act on the flow. Nevertheless, some preliminary results show that even if the solutal contribution is *a priori* small, it affects significantly the overall transfer. Further investigations are necessary to clarify this aspect.

6. Discussion

We have compared an analytical model predicting the influence of buoyancy convection on the measurement of diffusivities in the long capillary technique with experimental results. The model seems to provide a good understanding of these effect and moreover, it has been seen that a steady

magnetic field could help significantly to reduce convective effects. In the thermal buoyancy driven case, an exact analytical solution (erf function) can be found to the axial effective diffusion problem. In the solute buoyancy driven case, a one-dimensional unsteady non linear equation should be solved numerically in general.

The experimental results shown for the SnBi alloy confirm the analysis. A significant reduction of the apparent solute transfer has been demonstrated when a magnetic field is applied. For small convective levels, the convective contribution to the effective diffusivity varies as $(Gr\,Sc)^2/Ha^4$. This model can be useful in practice, to determine what magnetic field magnitude is necessary to provide experimental results with negligible convective contribution. With a $0.75\,T$ magnetic field, the Hartmann number achieved is 55 for a $2\,mm$ diameter capillary. At this Hartmann number, it is believed that the measured diffusivity is close to the actual diffusivity to a factor 1.3 for the SnBi alloy. According to the Ha^{-4} law, a slight increase in the magnitude of the magnetic field should permit us to measure correctly the diffusion coefficient.

Other configurations should be studied, like the vertical capillary (BG96). In that case, solute buoyancy forces can provide a stabilizing effect, instead of the driving effect here. This vertical configuration is extensively used in practice. The question to address is what should be the combined effect of the solute stabilization and a possible magnetic damping.

A general aspect concerning the use of a magnetic field to damp convective effects is related to the thermoelectric effect (MGKF96). If the crucible is not electrically insulating, electric currents of thermoelectric origin exist and generate a driving force when a magnetic field is applied.

Finally, it was suggested (YCC64) that a magnetic field could change the diffusivity as a physical property; however, it is not clear whether the experiments mentioned showed a true variation of D or a magnetic damping of an initially unexpected convection.

Acknowledgment: this work has received support from the CNES under the contract 97/CNES/071/6881.

References

T. Alboussière, J.P. Garandet, and R. Moreau. Buoyancy-driven convection with a uniform magnetic field. Part I. Asymptotic analysis. *J. Fluid Mech.*, **53** :545–563, 1993.

J.I.D. Alexander, J.F. Ramus, and F. Rosenberger. Numerical simulations of the convective contamination of diffusivity measurements in liquids. *Microgravity science and technology*, **9** :158–162, 1996.

A. Bejan. *Convection Heat Transfer.* Wiley and sons, 1984.

C. Barat and J.P. Garandet. The effect of natural convection in liquid phase mass transport coefficient measurements: the case of thermosolutal convection. *Int. J. Heat Mass Transfer*, **39**:2177–2182, 1996.

J.P. Garandet, T. Alboussière, and R. Moreau. Buoyancy driven convection in a rectangular enclosure with a transverse magnetic field. *Int. J. Heat and Mass Transfer*, **35**(4):741–748, 1992.

J.P. Garandet, C. Barat, and T. Duffar. On the effect of natural convection in mass transport measurements in dilute liquid alloys. *Int. J. Heat Mass Transfer*, **38**:2169–2174, 1995.

J.P. Garandet, J.P. Praizey, S. Van Vaerenbergh, and T. Alboussière. On the problem of natural convection in liquid phase thermotransport coefficients measurements. *Phys. Fluids*, **9**(3):510–518, 1997.

J.E. Hart. On sideways diffusive instability. *J. Fluid Mech.*, **49**:279–288, 1971.

D. Henry and B. Roux. Three-dimensional numerical study of convection in a cylindrical thermal diffusion cell: its influence on the separation of constituents. *Phys. Fluids*, **29**:3562–3572, 1986.

G. Mathiak, A. Griesche, K.H. Kraatz, and G. Frohberg. Diffusion in liquid metals. *Journal of non-crystalline solids*, **207**:412–416, 1996.

J.P. Praizey. Benefits of microgravity for measuring thermotransport coefficients in liquid metallic alloys. *Int. J. Heat Mass Transfer*, **32**(12):2385–2401, 1989.

W.V. Youdelis, D.R. Colton, and J. Cahoon. On the theory of diffusion in a magnetic field. *Canadian Journal of Physics*, **42**:2217–2237, 1964.